SPECTROSCOPIC STUDY OF ADSORBED CO AT POLYCRYSTALLINE COPPER IN AQUEOUS PHOSPHATE BUFFERED SOLUTION

Jumat Salimon

School of Chemical Sciences and Food Technology, Universiti Kebangsaan Malaysia,
43600 Bangi, Selangor DE, Malaysia

Abstract - The behavior of adsorbed CO at polycrystalline copper surface was investigated by infrared spectroscopy. It was found that the linear adsorbed CO, $Cu-CO_L$ was a dominant species on copper surface at low CO concentration. $Cu-CO_L$ was electrochemically converted to bridge bonded CO, $Cu-CO_B$ at high CO concentration. Increasing the CO surface coverage, θ_{CO} will increase the formation of adsorbed bridge bonded CO. N_2 purging treatment was used to examine the stability of the adsorbed CO through the evacuation process. The $Cu-CO_B$ remained intact while $Cu-CO_L$ was completely removed from the copper surface. It suggests that $Cu-CO_L$ may involve in a weak bonding to a copper surface such as in a physisorbed interaction, while $Cu-CO_B$ consists much stronger bonding such as a chemisorbed interaction. The N_2 purging treatment also gave an additional proof that $Cu-CO_B$ was partly converted to copper(I)-carbonyl, Cu(I)-CO at anodic potential regions.

Abstrak – CO terjerap di atas permukaan tembaga polikristal telah dikaji dengan spektroskopi inframerah. Hasil kajian menunjukkan pada kepekatan CO yang rendah CO terjerap secara linear, $Cu-CO_L$ merupakan species yang dominan. $Cu-CO_L$ bertukar secara elektrokimia ke bentuk CO terjerap secara jambatan, $Cu-CO_B$ pada kepekatan CO yang tinggi. Penambahan penurapan permukaan CO, θ_{CO} akan menambahkan kadar pembentukan CO terjerap secara jambatan. Kestabilan CO terjerap telah diuji secara pengolahan penyahjerapan melalui proses alih tukar gas N_2. $Cu-CO_B$ didapati masih kekal sementara $Cu-CO_L$ telah tersingkir keseluruhannya dari permukaan tembaga. Ini mencadangkan bahawa pembentukan $Cu-CO_L$ melibatkan ikatan secara lemah ke atas permukaan tembaga seperti jerapan fizik, manakala $Cu-CO_B$ terlibat dengan ikatan yang kuat seperti jerapan kimia. Pengolahan alih tukar gas N_2 telah memberikan bukti tambahan $Cu-CO_B$ telah tertukar ke bentuk tembaga(I) karbonil, Cu(I)-CO pada julat keupayaan anodik.

Key wors: Adsorbed carbon monoxide, polycrystalline copper, FTIR
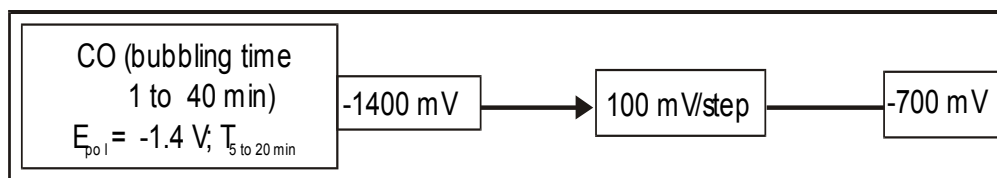
Introduction

The Blyholder model of metal-CO bonding is commonly used to rationalize the red shift in infrared spectrum of adsorbing CO frequency relative to its gas phase. The subsequent increasing in IR frequency as the CO coverage increases is due to a decrease in π back-bonding character [1]. This is usually associated with the donation of *d* electrons from the metal and this form can be used to explain the upward or downward chemical shift of $\nu C{\equiv}O$ on metals. The first component involves the main bonding between CO and the metal. This is a σ bonding interaction due to the overlap of a filled 5σ, "lone pair" orbital on the carbon atom with an empty metal *d*-orbital of the correct symmetry to form a dative type bond. In this classical theory, the σ–dative interaction leads to an excess electron density transfer from the CO molecule to the metal centre, thus the bond is repulsive. However polarization of the metal valence electrons away from the CO reduces this repulsion [1,2]. Therefore, due to the large formal negative charge on the metal, a π–back donation from a metal $d\pi$-orbital to the antibonding $2\pi^*$ molecular orbital on the CO ligand occurs to remove the excess negative charge. This is the second component of M-CO bonding and it involves a balancing of the excess charge. Donation of metal d electron forms a π bonding interaction due to the overlap of filled metal $d\sigma$ (e.g. $3d$ of copper) orbital with the $2\pi^*$ antibonding molecular orbital of CO, thus stabilizing the σ–dative bond. The π–back donation in M-CO is in the form of a simple Hückel molecular orbital where the wave function for the lowest orbital, P_1 places most of the charge on the carbon and oxygen atoms and adds to the bond strength for both the carbon-oxygen and metal-carbon bonds. However, the second orbital, P_2 whose energy is lower than a metal d-orbital, is "bonding" for the metal-carbon bond but "antibonding" for the carbon-oxygen bond, since the wave function has a node between the carbon and oxygen atoms.

On polycrystalline Cu (evaporated film in particular), consisting of micro crystallites of various orientations, so that the surface consists of a collection of microscopic high-index crystal faces. The infrared bands for metal-CO lie in the frequency range of approximately 2090 - 2110 cm^{-1} so that an ensemble of such faces could show a broad band. Low index surfaces on the other hand give bands at appreciably lower frequency at 2076 cm^{-1} on Cu(111) and at 2080 cm^{-1} on Cu(100) [3]. Frequency shifts with coverage occur on both single crystal surfaces but are very small and may be of either sign. Dipole coupling is expected to cause an upward frequency shift with respect to the surface coverage. Chemical effects, such as competition for the electrons involved in synergetic σ and π–bonding may cause shifts of either sign. Therefore it is very difficult to predict the magnitude of these shifts, which may be determined by isotopic decoupling. By varying the composition from a dilute mixture of ^{12}CO and ^{13}CO to pure ^{12}CO, it is possible to demonstrate a significant shift in frequency as the coverage increases arising from coupling interactions rather than chemical effects, which would be independent of isotopic composition [3,4].

In this work, the spectroscopic properties of adsorbed CO at polycrystalline copper surface was investigated when the CO surface coverage was varied by varying the polarization potential, the polarization time or by changing the concentration of CO in solution. The stability of the adsorbed CO band was also examined. Using the *in situ* IR measurements, the behavior of the adsorbed CO bands shifting, bands transformation and the bands stability on the copper surface are reported.

Experimental

The copper electrode used was electrochemically polished. First, the electrode was polished with successively down graded sizes up to 0.05 μm alumina powder, cleaned in ultrasonic bath prior to the electrochemical polishing. Experimental details in the present study have been reported elsewhere [5]. Electrochemically polished copper electrodes used throughout this work were cathodically protected by applying a negative potential immediately after its immersion into degassed phosphate buffered solution (pH 6.8). A cathodic potential, which is close to or at the hydrogen evolution potential was applied for few minutes before the cyclic voltammetry measurements in order to remove any oxides or hydroxides from the surface. Nitrogen gas was bubbled through the solution between the experiments and passed over the electrolyte quiescently during experiments. Carbon monoxide was bubbled for 15 minutes to prepare CO-saturated solutions for the CO adsorption experiments. The IR spectral measurements were performed in a staircase mode using a fully evacuated FTIR spectrometer (Bruker IFS-113V) fitted with a mercury-cadmium-telluride (MCT) photoconductive detector cooled at 77 $^{\circ}$K (using liquid nitrogen), *p*-polarizer and Ge/KBr beam splitter. The optics bench was fully evacuated. Medium resolution (4) was sufficient for Substractively Normalized Interfacial Fourier Transform Infrared Spectroscopy, SNIFTIRS experiments and this was attainable throughout the mid-IR region, with a maximum aperture of 10 mm diameter and medium scanner speed of 6 kHz/sec. SNIFTIR spectra collection was performed at 200 scan in a staircase mode. The potential, either generated by Hi-Tek DT-2101 potentiostat and PP-R1 waveform generator, was changed by 100 mV during each step or from a custom written software for an interface digital to analogue converter (DAC), which was run under OPUS 3.0, which enables voltage 'steps' to be programmed. The DAC conveyed a programmed voltage sequence to the potentiostat (HI-TEK DT2101). A time delay can be introduced after any change in voltage and before the collection of spectra was started, in order to allow the electrochemical system to reach a stable semi-steady state.

Figure 1: Scheme A used to evaluate the adsorption of CO on Cu

In order to investigate the influence of θ_{CO} on the adsorption of CO on copper surface, a series of experiments were performed at a fixed E_{pol} = -1.4 V. The electrode was introduced into N$_2$-saturated solution and held at open circuit potential. Carbon monoxide was then bubbled into solution for 1 min. A

potential of -1.4 V was then applied for varying periods of time or holding time, $T_{hold\ min}$, and the electrode was pushed against the IR transparent window after which spectral collection was performed. The potential was then stepped in 0.1 V increments to -0.7 V following Scheme A in Figure 1. The electrode was then removed from solution, electropolished and reintroduced into a N_2 saturated solution. CO was bubbled for the same period of time and the electrode was polarized at the same potential for a longer period of time, $2T_{hold\ min}$, pressed against the IR window and then the spectra were collected. The procedure was repeated for different polarization time, e.g. t_5, t_{10}, t_{15} to t_{20}.

Result and discussion

The effect of CO surface coverage

Figure 2 (A) shows the SNIFTIR spectra at -0.8 V (normalized relative to -1.4 V), obtained when the bubbling time of CO was 1 min and $T_{hold\ min}$ varied up to 20 min. The spectra show that after 5 min of polarization time (Fig 2 A t_5), Cu-CO$_L$ (Fig 3A) is replaced by Cu-CO$_B$ (Fig 3B). As t_x increases, Cu-CO$_B$ shifts to higher frequencies (Fig 2 A t_{20}). Increasing the concentration of CO by bubbling for 3 min has the same effect on Cu-CO$_L$/ Cu-CO$_B$ conversion (Fig 2 B). However the increased intensity of the Cu-CO$_L$ band (positive band at 2080 cm^{-1}) indicate that more Cu-CO$_L$ is present at the surface under these conditions (E_{pol} = -1.4 V, bubbling time = 3 min) compared to the same potential but at a CO bubbling time of 1 min. Furthermore, the intensity of Cu-CO$_B$ is higher at 3 min bubbling time of CO and the band further shifts to higher wave numbers. The same trend is observed for varying bubbling times (10, 15, 20, 25, 30, 40 min; for the sake of clarity only the 15 and 40 min experiments are shown); however the amount of Cu-CO$_L$ starts to decrease after 15 min of bubbling time, even though the amount of Cu-CO$_B$ continues to increase. The reason for the apparent reduction in the amount of Cu-CO$_L$ is possibly due to the molecules moving into a tilted position. Raval *et al.* [6] reported that adsorbed CO shifts from linear to tilted linear as θ_{CO} increases. As *p*-polarized radiation probes vibrations, which have a dipole moment perpendicular to the surface, a tilt in Cu-CO$_L$ results in a decreased vector of the dipole moment which is perpendicular to the surface, hence the decrease in the Cu-CO$_L$ peak area with bubbling time.

It is interesting to note that the time taken to bubble CO in the solution affects the Cu-CO$_L$ peak area due to the conversion towards the more stable of adsorbed CO. The conversion of Cu-CO$_L$ to Cu-CO$_B$ is expected and best examined looking at Fig 2 C ($t_{bubbling}$ = 15 min), which shows that the amount of Cu-CO$_L$ decreases whereas Cu-CO$_B$ increases with holding time. This implies that as the θ_{CO} increases (due to an increase in the amount of CO in solution and the increased holding time), Cu-CO$_B$ is preferentially formed. This indicates that the preference of the adsorbed CO binding site on the polycrystalline copper electrode is at linearly binding site follow by multiple binding sites of bridge bonded. This might due to the preference of the Cu/CO orbital interaction. The bonding process in adsorbed CO on Cu involves the interaction between the overlap of copper *d* orbital and the highest occupied CO 5σ orbital [7]. Persson *et al.* reported that the orbital overlap between the copper-5σ orbital interactions is larger in linear bonded and smaller in bridge bonded bonding. Therefore energetically the linear bonded site is a preference adsorption site and will be occupied first followed by the bridge-bonded site, with increasing CO coverage. The Cu-5σ orbital interaction is believed to be more important compared to other possible orbital interaction such as the copper-2π* orbital. At longer polarization time, Cu-CO$_L$ rearranged and adsorbed at bridge binding site, possibly induced by the change of the electronic energy levels [8,9] as the orbital interaction of Cu-5σ decreases, as the CO coverage increases.

The frequency shift to higher wave numbers in the Cu-CO$_B$ brought about by increased holding and bubbling times can be partly explained in terms of the repulsive strain among the adjacent neighboring Cu-CO$_B$ molecules. To reduce the steric strain effect of this repulsive force, a shift of binding sites toward other possible defect 2-fold binding sites such as 2-fold step or 2-fold terrace binding sites might occur. Therefore an increase in θ_{CO} may result in the formation of more Cu-CO$_B$ at step or terrace binding site, thus increasing the band frequency position due to these defect binding sites producing stronger CO bonding compared to normal bonding sites due to their more unsaturated or lower coordination binding sites [10,11]. It has been found that adsorbed molecules at step sites do indeed exhibit different frequency from those on terraces. Copper step sites give rise to bands at about 15 cm^{-1} higher than those of terrace sites [12,13,14,15]. Therefore increasing the CO concentration (increase θ_{CO}) gives rise to higher CO$_B$ band frequency, from 1882 cm^{-1} (1 minute of CO bubbling time) to 1918 cm^{-1} (40 minute of CO bubbling

time).   In addition, this frequency shift can also be explained by classical π-back donation where a decrease in back donation to CO antibonding orbital occurs as θ_{CO} increases due to high competition for metal d electrons, thus increasing the $\nu C\equiv O$ stretching frequency.   Increases in θ_{CO} also leads in dipole-dipole coupling interaction among the adjacent neighboring CO molecules, thus increases the $\nu C\equiv O$ stretching frequency [16].
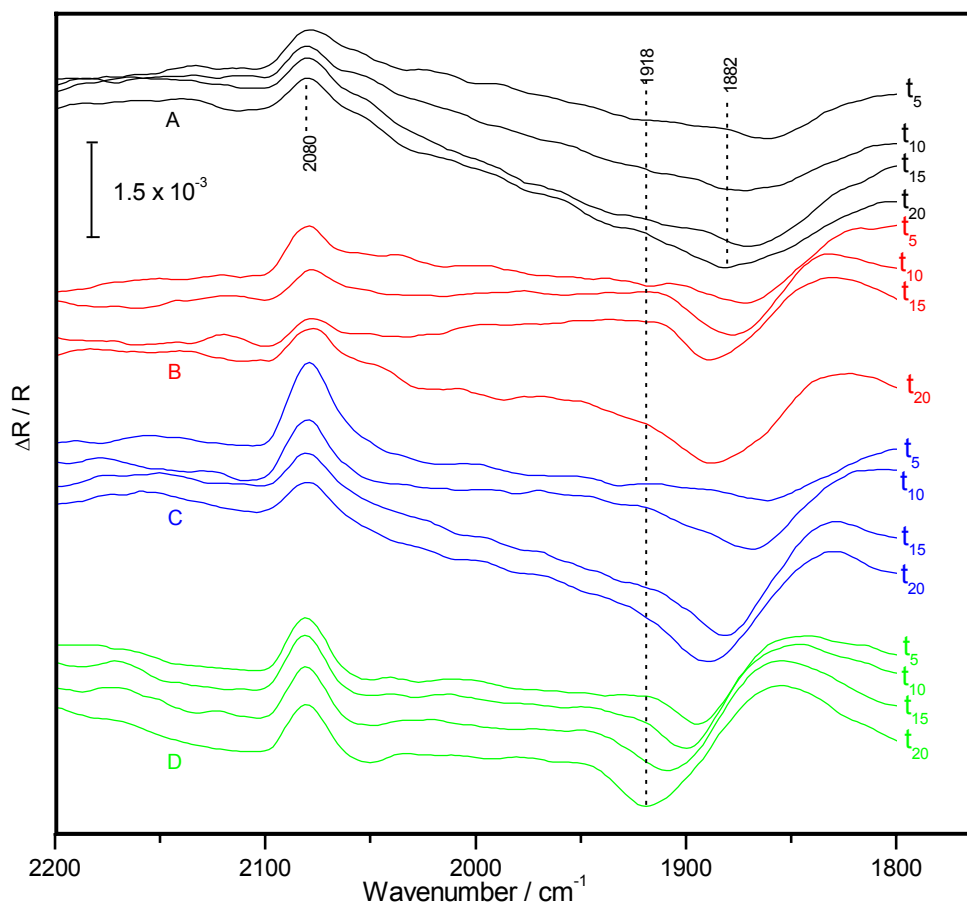
Figure 2: SNIFTIR spectra at –0.8 V obtained from different CO concentration/CO bubbling time; A (1 min), B (3 min), C (15 min) and D (40 min) in buffered phosphate solution. The electrode was polarized at E_{pol} = –1.4 V for different holding time; t_5 (T_{hold} = 5 min), t_{10} (T_{hold} = 10 min), t_{15} (T_{hold} = 15 min) and t_{20} (T_{hold} = 20 min). Spectra are normalized relative to spectrum obtained at –1.4 V of each set.

Stability of the adsorbed CO

The bond strength, in particular of adsorbed intermediate species, is relatively important to their reactivity. If the bonding between an adsorbed intermediate and the electrode is strong, it will affect the intermediate reactivity by slowing down the next step in the reaction. A weaker bond on the other hand might lead to higher reactivity. A typical example of this is the hydrogen evolution reaction in which the rate and mechanism of gas evolution depends on the metal-H bond strength.   Physical evacuation processes are ways to evaluate the CO adsorbed bond strength on copper surfaces (mainly in UHV studies).   Purging the adsorbed CO from the electrode surface by an inert gas is another way of achieving this in electrochemical systems. Experiments were carried out by polarizing the electrode surface at E_{adm} of –1.4 V for 15 minute in CO-saturated phosphate buffered solutions to form both linearly and bridge bonded adsorbed CO. The spectra were recorded as the potential is stepped down to –0.8 V in 0.1 V/step as shown by Scheme B in

Figure 4. The electrode was lifted from the window and the potential was then slowly brought back to the initial E_{adm} of -1.4 V to restore both Cu-CO$_L$ and Cu-CO$_B$. The solution was then purged with N$_2$ gas for 30 minutes to remove any CO from the solution and then the spectra were recorded as the potential was stepped down to –0.8 V as before.
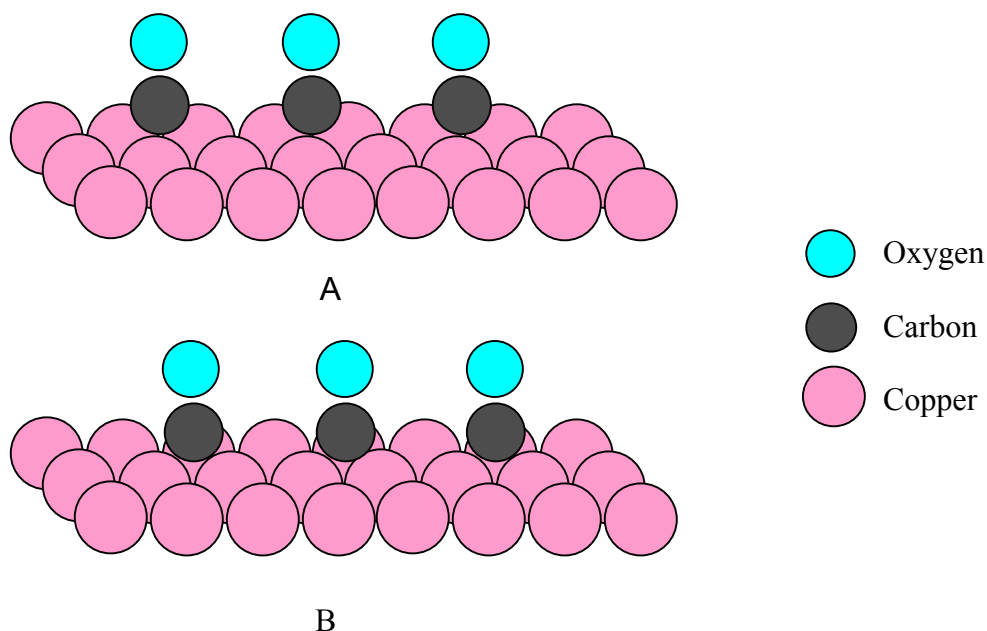

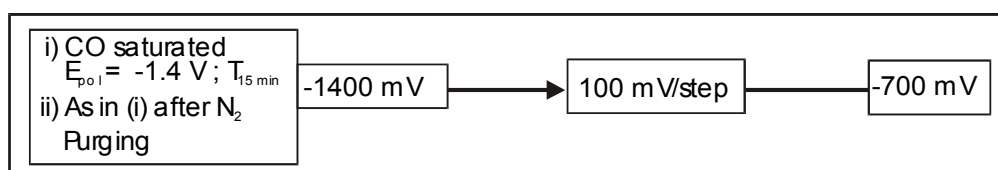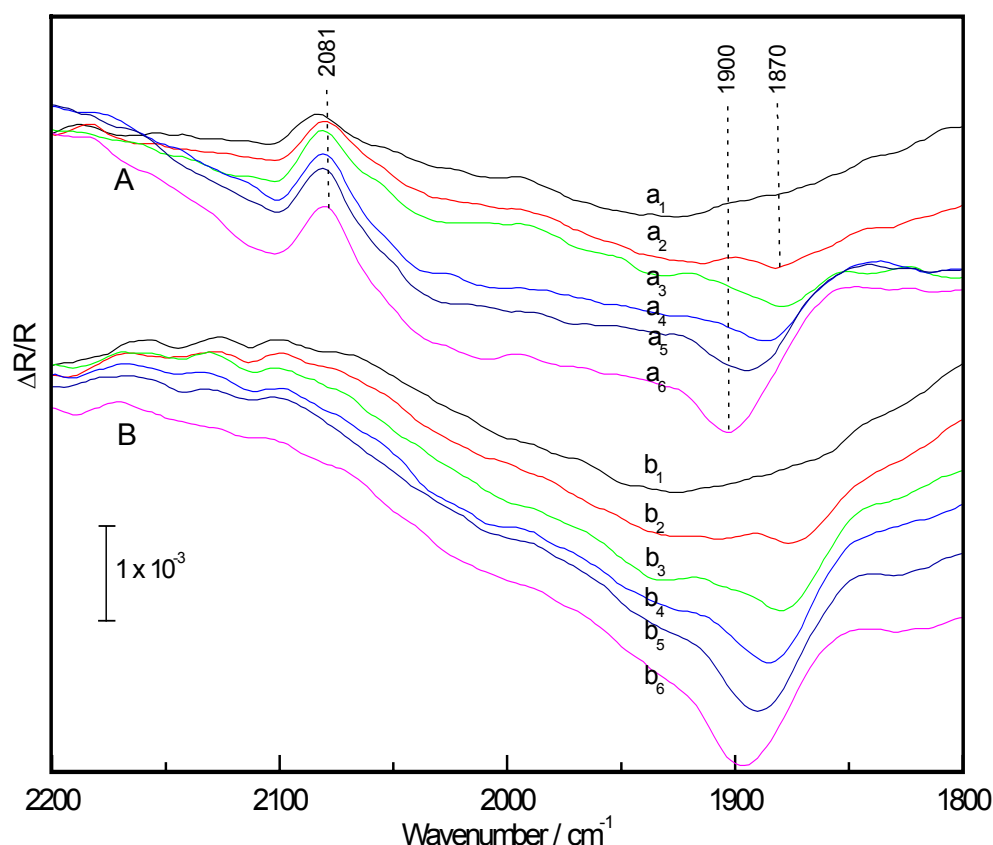**Figure 3**: Schematic illustration of Cu-CO$_L$ (A) and Cu-CO$_B$ (B).

Figure 4: Scheme B used to evaluate the adsorption of CO on Cu

Figure 5: SNIFTIRS spectra obtained from CO-saturated buffered phosphate solution (A) before and (B) after N_2 purging. Spectra shown are from (1) –1.3 V to (6) –0.8 V; normalized relative to –1.4 V.

Figure 5 shows the SNIFTIR spectra for both sets of experiments; (a) CO saturated and (b) N_2 saturated. The spectra are normalized relative to spectrum obtained at –1.4 V. The figure shows positive going band for Cu-CO_L at 2081 cm^{-1} and negative going band for Cu-CO_B at 1870 cm^{-1} for the CO-saturated solution before N_2 purging (spectrum a_1 to a_6), and total disappearance of the Cu-CO_L band and the retention of Cu-CO_B band at 1870 cm^{-1} after the N_2 purging (spectrum b_1 to b_6). The results indicate that Cu-CO_L is completely removed from Cu through the N_2 purging process whereas Cu-CO_B remains unchanged. This indicates that Cu-CO_L is weakly adsorbed at Cu. This is in agreement with its relatively low dissociation energy of 30 kJ/mol (CuCO cluster system) as reported by Schwerdfteger and Bowmaker [17]. They suggested that Cu-CO interaction is best described as combination of dispersion, donor-acceptor (charge transfer) and repulsive interactions. Furthermore this is well in agreement with other values of the binding energies of CuCO and Cu_2CO clusters calculated at about 25.1 kJ/mol and 104.6 kJ/mol respectively [18,19]. The difference in bond stability is also supported by the fact that Cu-CO_L only appears in a small potential range from –1.5 to –1.0 V, whereas Cu-CO_B can be observed over a wider potential range from –1.5 V to –0.1 V [20]. The increase in stability of Cu-CO_B compared to Cu-CO_L can be ascribed to the strengthening of bonding between Cu and CO by the increase of the π back donation of the *d* metal electrons into the $2\pi^*$ orbital through the two Cu-C bonds. The ease of Cu-CO_L removal from the surface by N_2 purging may suggest that it is weakly bonded or it might only physisorbed on Cu surface.

It is worth noting that after the N_2 purging process, Cu-CO_B remained unaffected and if the potential was further stepped down more positive potentials; the band at 2107 cm^{-1} appeared at –0.1 V. However the band intensity was much less compared to the band intensity when the experiment was carried out in CO saturated solution. This suggests that since the measurements were performed in the N_2 environment, the appearance of Cu(I)-CO must come from the only CO source available in the system, which is Cu-CO_B. This indicates that the interconversion of Cu-CO_B to Cu(I)-CO indeed occurs at the positive potential and

further reconfirms that Cu-CO$_B$ is converted to Cu(I)-CO at anodic potential. Figure 6 shows a "summary" of the stability of Cu-CO$_L$ (A$_1$ and B$_1$), Cu-CO$_B$ (A$_2$ and B$_2$) and Cu(I)-CO (A$_3$ and B$_3$) at three specific potentials. The stability of Cu-CO$_L$, Cu-CO$_B$ and Cu(I)-CO was also examined using a flow cell. As expected, Cu(I)-CO was removed from the thin layer during such experiments. Surprisingly, no Cu-CO$_L$ was observed during the imposition of a flow regime.

Conclusion

It is clear that the Cu-CO$_L$ becomes dominant adsorbed CO species on copper surface at low CO concentration. Cu-CO$_L$ is electrochemically converted to Cu-CO$_B$ at high CO concentration by bubbling CO in solution at least for 5 min. The results show that increasing the CO surface coverage will increase the formation of more stable adsorbed CO at bridge-bonded sites. It has been shown that Cu-CO$_B$ remains unchanged while Cu-CO$_L$ is completely removed from the copper surface through an inert gas purging. It suggests that Cu-CO$_L$ may involve in a weak-bonding interaction toward the copper surface such as physisorbed interaction, while Cu-CO$_B$ consists much stronger bonding such as chemisorbed interaction. At anodic potential regions Cu-CO$_B$ is partly converted to copper(I)-carbonyl, Cu(I)-CO, as the copper surface started to oxidized.

Acknowledgment
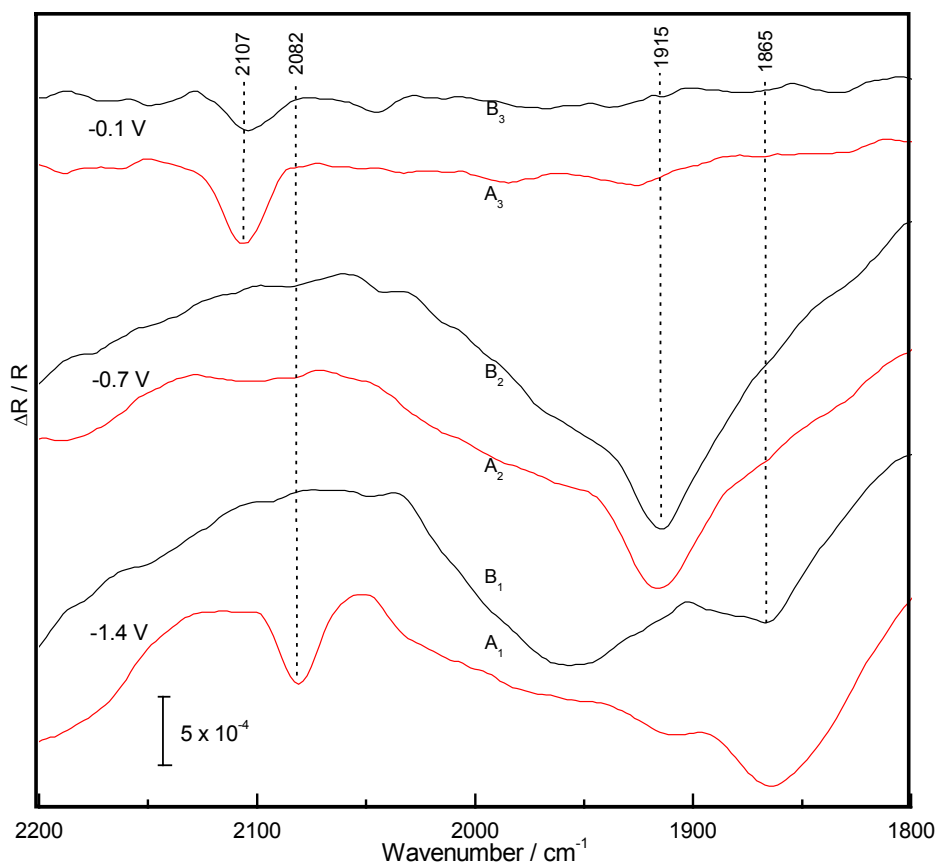
Figure 6: SNIFTIR spectra obtained from (A) before and (B) after N$_2$-purged buffered phosphate solution. Spectra shown are at −1.4 V (A$_1$ and B$_1$), −0.7 V (A$_2$ and B$_2$) and −0.1 V (A$_3$ and B$_3$), normalized relative to −0.4 V (reverse sweep).

References

1   G. Blyholder, *J. Phys. Chem.,* 1964, **68**, 2772
2   J.H.B. Chenier, C.A. Hampson, J.A. Howard and B. Mile, *J. Phys. Chem.,* 1989, **93**, 114
3   P. Hollins and J. Pritchard, *Vibrational Spectroscopy of Adsorbates*, Series in "Chemical Physics", 1980, vol. 15, Chp. 8.
4   P. Hollins and J. Pritchard, *Surf. Sci.*, 1983, **134**, 91
5   J. Salimon and M. Kalaji, *Malay. J. of Science,* 2001, **20**, 71.
6   R. Raval, S.F. Parker, M. E. Pemble, P. Hollins, J. Pritchard and M.A. Chesters, *Surf. Sci.*, 1988, **203**, 353
7   B.N.J. Persson, M. Tushaus and A.M. Bradshaw, *J. Chem. Phys.,* 1990, **92**, 5034
8   F. Kitamura, M. Takahashi and M. Ito, *J. Phys. Chem.,* 1988, **92**, 3320
9   H. Ogasawara, J. Inukai and M. Ito, *Chem. Phys. Let.,* 1992, **198**, 389
10   J.P. Biberian and M.A.Van Hove, *Surf. Sci.*, 1984, **138**, 361
11   C. Ruggiero and P. Hollins, *J. Chem. Soc., Faraday Trans*., 1996, **92**, 4829
12   P. Hollins, K.J. Davies and J. Pritchard, *Surf. Sci.*, 1984, **138**, 75
13   P. Dumas, R.G. Tobin and P.L. Richards, *Surf. Sci.*, 1987, **173**, 79
14   J. Pritchard, T. Catterick and R.K.Gupta, *Surf. Sci*., 1975, **53**, 123
15   E. Borguet and H-L. Dai, *J. Chem. Phys*., 1994, **101**, 9080
16   J-W. He, W.K. Kuhn, L-W.H. Leung and D.W. Goodman, *J. Chem. Phys*., 1990, **93**, 7463
17   P. Schwerdftfeger and G.A. Bowmaker, *J. Chem. Phys*., 1994, **100** 4487
18   M.A. Blitz, S.A. Mitchell and P.A. Hackett, *J. Phys. Chem.,* 1991, **95** 8719
19   R. Fournier, *J. Chem. Phys*., 1995 **102**, 5396
20   Jumat Salimon, Ph. D Thesis, 2001, University of Wales. ↵